

1 SARS CoV-2 nucleoprotein enhances the infectivity of lentiviral spike particles

2 Tarun Mishra^{*1}, Sreepadmanabh M^{*1}, Pavitra Ramdas¹, Amit K Sahu¹, Atul Kumar², Ajit
3 Chande^{1,3}

4 ¹ Laboratory of Molecular Virology, Department of Biological Sciences, Indian Institute of
5 Science Education and Research, Bhopal, India

6 ² Structural Biology Laboratory, Department of Biological Sciences, Indian Institute of Science
7 Education and Research, Bhopal, India

8 ^{*}Contributed equally

9 ³ Correspondence: Ajit Chande

10 **Corresponding author email:** ajitg@iiserb.ac.in

11 **Author contributions:** Performed research, analyzed data: TM, SM, PR, AKS, AC. Contributed
12 reagents: AK. Wrote the paper: AC, SM. Conceived, Designed research, Supervision: AC. All
13 authors have approved the final draft. Contributed equally: TM, SM

14 **Competing interest statement:** Authors declare no competing interests

15 **Keywords:** SARS-CoV-2; Virus Neutralization; Spike lentiviral pseudotyping; Nucleocapsid;
16 ACE2-Fc;

17

18 Abstract

19 The establishment of SARS CoV-2 spike-pseudotyped lentiviral (LV) systems has enabled the
20 rapid identification of entry inhibitors and neutralizing agents, alongside allowing for the study of
21 this emerging pathogen in BSL-2 level facilities. While such frameworks recapitulate the cellular
22 entry process in ACE2+ cells, they are largely unable to factor in supplemental contributions by
23 other SARS CoV-2 genes. To address this, we performed an unbiased ORF screen and
24 identified the nucleoprotein (N) as a potent enhancer of spike-pseudotyped LV particle
25 infectivity. We further demonstrate that this augmentation by N renders LV spike particles less
26 vulnerable to the neutralizing effects of a human IgG-Fc fused ACE2 microbody. Biochemical
27 analysis revealed that the spike protein is better enriched in virions when the particles are
28 produced in the presence of SARS CoV-2 nucleoprotein. Importantly, this improvement in
29 infectivity is achieved without a concomitant increase in sensitivity towards RBD binding-based
30 neutralization. Our results hold important implications for the design and interpretation of similar
31 LV pseudotyping-based studies.

32 Introduction

33 The ongoing coronavirus disease 2019 (COVID-19) pandemic has provided a strong impetus for
34 studies aimed at discovering and characterizing neutralizing antibodies or small molecule
35 inhibitors targeted against the severe acute respiratory syndrome coronavirus 2 (SARS CoV-
36 2). A major focus of these efforts has been the spike (S) glycoprotein of the virus, which
37 mediates the viral entry into target cells by recognition and binding to the cell-surface receptor
38 angiotensin-converting enzyme 2 (ACE2) ^{1,2}.

39
40 Numerous studies have demonstrated that the spike protein may be employed to generate
41 stably pseudotyped lentiviral, retroviral, and vesicular stomatitis virus particles ³⁻⁷. Given that
42 live SARS CoV-2 is a biosafety level-3 agent, these pseudotyping approaches have greatly
43 facilitated investigations undertaken within lower containment facilities. Importantly, this has also
44 allowed for the screening and characterization of neutralizing antibodies against SARS CoV-2,
45 as these primarily show reactivity against the spike protein ⁸. Furthermore, such pseudoviruses
46 are deployable as platforms for the large-scale screening of small molecule inhibitors and
47 pharmacological agents which possess therapeutic potential against COVID-19 ⁹.

48
49 In this regard, capitalizing on the interaction of the S protein with cellular ACE2, strategies have
50 been reported which utilize chimeric ACE2 fused to the Fc region of human IgG as a potent
51 neutralizing agent against spike-pseudotyped viruses ¹⁰. This arsenal now includes variations
52 such as mutations to the catalytic region of ACE2 (thereby preventing undesirable side-effects
53 during in vivo administration), and modified Fc domains ^{10,11}. However, a common feature of
54 these studies is that they invariably adopt pseudoviruses which are enveloped by spike, but do
55 not incorporate contributions from any other SARS CoV-2 genes.

56
57 This point is particularly crucial in light of the manifold roles adopted by various genes of the
58 SARS CoV-2, as has been highlighted in recent interactome studies ^{12,13}. Indeed, the specific
59 effects of these genes continue to be investigated and represent a wide diversity of specialized
60 functions. Building on this, we hypothesized that specific genes of the SARS CoV-2 could play a
61 key role in enhancing the infectivity of viral particles. To probe this, we undertook an unbiased
62 screen of twenty-four ORFs, NSPs, and structural protein genes of the SARS CoV-2 using
63 spike-pseudotyped lentiviral particles. Our observations implicated the N protein as an enhancer

64 of viral infectivity. We further show that this enhancement of infectivity renders the viral particles
65 less sensitive to ACE2-Immunoglobulin chimera-mediated neutralization.

66

67 **Results**

68

69 A custom-designed transfer vector (**Fig. 1A**), termed pScalps Luciferase-Zsgreen, as well an
70 ACE2-expressing HEK293T cell line (**Fig. 1B**) were generated for this study. To investigate the
71 effect of various SARS CoV-2 genes on viral infectivity, we undertook an unbiased screen, as
72 outlined by the schematic in **Fig. 1C**. Briefly, HEK293T producer cells were transfected with
73 plasmids encoding the codon-optimized S protein (with a nineteen amino-acid deletion at the C
74 terminal), the packaging plasmid psPAX2, and the pScalps Luciferase-Zsgreen reporter
75 plasmid. Alongside this, each one of the twenty-four SARS CoV-2 genes was separately co-
76 transfected with the above.

77

78 ACE2-expressing HEK293T cells were transduced with viruses produced in the presence of
79 indicated SARS CoV-2 genes, and the extent of infectivity was gauged as a measure of both
80 GFP-positive cell count and firefly luciferase unit's assessment 48 hours post-infection (**Fig.**
81 **2A**). Expression of all the SARS CoV-2 genes was verified at the RNA level and the effect of
82 this expression was also checked on the lentiviral capsid levels by western blotting from the
83 producer cell lysates (**Fig. 2B and 2C**). Based on this screen, we identified the nucleocapsid (N)
84 protein as an enhancer of spike-pseudovirus infectivity. We scored the effects on infectivity in
85 conditions where the co-expression of SARS CoV-2 genes increased the infectivity without an
86 apparent effect on the lentiviral capsid levels (**Fig. 2C**). The particle infectivity enhancement by
87 N was also discernible with a GFP reporter suggesting this assay reliably measures
88 transduction events (**Fig. 2D**). The infectivity-enhancement effect of N was not observed in the
89 case of VSV-G pseudotyped lentiviral particles (**Fig. 2E**). Cumulatively, these results appear to
90 implicate the viral N protein as an intrinsic enhancer of lentiviral spike-pseudotyped particle
91 infectivity.

92

93 Next, we asked if such an enhancement of particle infectivity would impact the ability of
94 neutralizing agents to block these particles from infecting host cells. Capitalizing on the
95 interaction of the S protein with cellular ACE2, we generated a SARS CoV-2 entry receptor-
96 based synthetic microbody consisting of a soluble ACE2 domain fused with the Fc region of
97 human IgG (**Fig. 3A**), which also carried a C-terminal 6XHistidine tag. Extracellular expression,

98 as well as the ability of ACE2-IgFc to dimerize under the experimental conditions that retained
99 disulphide linkage, were detected by Western blotting (**Fig. 3B**). These experiments also
100 confirmed the presence of an intact Histidine tag. Furthermore, we tested the specific interaction
101 of the ACE2-IgFc with spike-pseudotyped LV particles by a pull-down experiment wherein the
102 on-bead capture of viral particles using protein G-bound ACE2-IgFc resulted in a ~10,000-fold
103 enrichment of spike pseudotyped viruses over VSV-G pseudotyped or non-enveloped (bald)
104 lentiviral particles (**Fig. 3C**). This also suggests that Fc configuration remained intact after fusion
105 with ACE2 thereby facilitating the immobilization of the microbody on the protein G magnetic
106 beads for virion capture. In sum, these results established that the ACE2-IgFc molecule is stably
107 expressed and demonstrates a high affinity specifically towards the S glycoprotein-laden
108 particles.

109
110 Following this, we wished to ascertain the relative titer of ACE2-IgFc required to effectively
111 restrict the infection of ACE2+ target cells, under the influence of the N protein. Briefly, lentiviral
112 particles either pseudotyped with S protein (with and without co-transfection with N) or bald
113 particles lacking envelope were generated, normalized to the RT units, incubated with ACE2-
114 IgFc according to the indicated concentrations, and used to transduce ACE2+ HEK293T target
115 cells. Luciferase activity assay, as a quantitative and sensitive indicator of transduction events,
116 revealed the ability of ACE2-IgFc to impair the infectivity of spike pseudotyped viruses in a
117 dose-dependent manner. Furthermore, results obtained herein demonstrate the requirement for
118 at least one log higher neutralizing titer of ACE2-IgFc microbodies in the case of N-enhanced
119 particles as opposed to those generated solely by the spike glycoprotein in order to elicit similar
120 levels of inhibition (**Fig. 4A**). The higher requirement of neutralizing agent was not a result of
121 higher particle counts as the inoculum was normalized to the reverse transcriptase units prior to
122 the target cell challenge.

123
124 Based on this, we envisaged a modification of virus particles by N that plausibly impacted the
125 virion quality, rather than the quantity. To better understand this, we asked if N protein directly
126 impacted the spike protein itself in order to effect infectivity enhancement. Accordingly, the viral
127 particles produced under indicated conditions were pelleted on a sucrose cushion as described
128 earlier¹⁴. Biochemical analysis of the virus pellet and the corresponding cell lysates by Western
129 blotting revealed that while N modestly improved the steady-state levels of spike in the producer
130 cell lysates, the spike signal was noticeably more prominent from the virions (**Fig. 4B**). The
131 augmentary effects of N appear to be specific in nature, given that exclusively lentiviral

132 components do not show any apparent changes in expression. Altogether, these experiments
133 indicated that N protein likely enhances the incorporation of spike protein into the virions,
134 thereby improving the particle quality and its infectivity.

135

136

137 **Discussion**

138

139 Considering the technical difficulties associated with studying live, replication-competent native
140 SARS CoV-2, the adoption of lentiviral or retroviral pseudotyping-based systems has enabled a
141 more widespread and accessible investigation of this pathogen. Significant advances have been
142 achieved in recent times, ranging from optimization of pseudotyping protocols to the application
143 of these for screening entry inhibitors ⁹. The roles of structural proteins such as M, E, and N in
144 assisting viral assembly and particle formation have also been explored ⁶. Along similar lines,
145 leading studies have deciphered the manifold cellular associations and interactions of various
146 SARS CoV-2 genes, in processes as diverse as host translation inhibition, disruption of splicing,
147 immune evasion, and protein trafficking, among others ¹⁵⁻¹⁸.

148

149 In the present study, we have evaluated the potential of twenty-four SARS CoV-2 genes to elicit
150 superior infectivity levels as compared to what may be achieved by mere pseudotyping with the
151 spike glycoprotein. Chief among these has been the nucleocapsid (N) protein. While a previous
152 study has established the crucial role played by N in viral genome processing and nucleocapsid
153 assembly ¹⁹, to the best of our knowledge there have been no prior reports specifically
154 highlighting its ability to elevate lentiviral spike pseudovirus infectivity.

155

156 An interesting parallel here is the recent report that the emerging dominant D614G spike mutant
157 is, regardless of the increased infectivity, rendered more susceptible to neutralization ²⁰. In
158 direct contrast, here we observe an alternate scenario at play - albeit within the restricted
159 context of lentiviral pseudotypes. Our assessment of spike pseudotyped viruses generated from
160 both N-exclusive and N-inclusive backgrounds indicates that the latter requires a higher
161 neutralizing titer of chimeric ACE2-IgFc molecules to effectively restrict infection of ACE2+ cells.
162 This directly implicates N as a potent enhancer of virion quality and infectivity, without an
163 accompanying increment in vulnerability towards RBD binding interactions-based neutralizing
164 agents. The evidence pointing towards the enrichment of spike glycoprotein within viral fractions
165 in an N-dependent manner lends support to this hypothesis. Set against the backdrop of recent

166 reports which highlight how specific mutations in the spike glycoprotein significantly bolster
167 infectivity²¹, the identification of N in this particular role may be a telling example of how the
168 SARS CoV-2 adopts a host of varied and as-yet incompletely explored strategies to drive its
169 pathogenesis.

170
171 In sum, our results underscore the importance of factoring in additional contributions from the
172 other viral genes while undertaking lentiviral vector pseudotyping with the spike glycoprotein of
173 the SARS CoV-2. While existing studies have managed to develop and validate platforms for
174 the screening of neutralizing antibodies and inhibitory chemical compounds, we believe that our
175 results highlight the necessity of incorporating additional genetic elements which have been
176 shown to boost viral infectivity. Furthermore, putative therapeutic candidates currently being
177 scrutinized in various clinical studies would benefit from lentiviral pseudotyping assays that
178 incorporate additional virion components during the large-scale screening stage.

179

180 **Methods**

181

182 **Cell culture**

183 HEK293T (from ATCC) were cultured in DMEM containing 10% Fetal Bovine Serum (US origin
184 certified serum, 1% penicillin-streptomycin and 20mM L-glutamine (complete medium), all
185 obtained from Gibco. The ACE2 expressing stable HEK293T cell line was generated by
186 transduction with lentiviral particles followed by selection with hygromycin until the entire non-
187 transduced population was eliminated. Expression of ACE2 was verified as described below.

188

189 **Plasmids**

190 The list of plasmids that were used in this study is provided below (refer to “Table S1: List of
191 Plasmids”) and are available upon a reasonable request. pScalps-Luciferase-Zsgreen was
192 generated by cloning a firefly luciferase gene that was PCR amplified with primers incorporating
193 the XhoI/EcoRI restriction sites. The resultant PCR product was digested and ligated in the
194 pScalps ZSgreen plasmid using identical sites and the inserts were confirmed by Sanger
195 sequencing.

196 ACE2 expressing lentiviral plasmid was generated by amplifying ACE2 encoding gene from the
197 Addgene plasmid #154987 and cloned into a modified pScalps lentiviral vector carrying the
198 hygromycin selection marker. SARS CoV2 encoding genes (detailed below in “Table S1: List of
199 Plasmids”) were generously provided by the Nevan Krogan Lab in the lentiviral backbone pLV-

200 TetONE, which were further subcloned into a non-viral pcDNA based custom-designed vector
201 for expression of these gene in transient transfection assays. After cloning, each gene of
202 interest preserved the Strep tag in-frame at the C-terminus.

203 All the oligos for generation/sequencing of the plasmids used in this study were custom
204 synthesized by Sigma Aldrich.

205

206 **Lentivirus production and quantification**

207 In general, lentiviral particles were produced by calcium phosphate transfection of HEK293T
208 with 8 µg of transfer vector, 6 µg of packaging plasmid (psPAX2) and 2 µg of envelope plasmid
209 (spike-expressing plasmid or pMD2.g for virus pull-down assay). The culture medium was
210 replaced at 16h-post transfection. Lentiviral vector-containing supernatant was collected 48h
211 after transfection and was centrifuged and filtered through 0.22 µm syringe filters. The infectivity
212 assay was performed after normalizing reverse transcriptase (RT) units obtained from an
213 SGPRT assay as described earlier¹⁴. Briefly, the target cells were infected in quadruplicates
214 (or at least triplicate) with up to 125-fold dilutions and the infectivity was acquired from the
215 dilutions in the linear range as reported previously¹⁴. Expression of GFP or Luciferase as a
216 quantitative measure of infection was acquired using Spectramax plate reader or CX7 High-
217 content imaging platform (CellInsight CX7 High Content Screening platform, ThermoFisher
218 Scientific and SpectramaxI3X, Molecular Devices, USA).

219 The SARS CoV-2 genes' screen was performed by producing spike pseudotyped lentiviruses
220 from HEK293T cells that were seeded in 12-well plate. Next day cells were transfected with
221 pScalps luciferase ZSgreen (800 ng), psPax2 (600 ng), spike expression plasmid (200 ng), and
222 either vector control or ORF carrying vector (300 ng) by the calcium phosphate method. Culture
223 medium was replaced with fresh medium 16h after transfection. Spike pseudotyped viruses
224 were collected after 48h of transfection. Supernatant was collected and centrifuged at 1200Xg
225 for 5 min and filtered using a 0.22 µm syringe filter.

226 Spike pseudotyped viruses were then used to transduce ACE2 expressing HEK293T cells to
227 check the infectivity level by either by GFP positive cell count and or by Luciferase assay.

228 To quantify the RT units, 5 µl viruses were lysed in a 5 µl lysis buffer and diluted with a core
229 buffer to make volume 100 µl. A 10 µl diluted viral lysate was mixed with an equal volume of 2X
230 reaction buffer and the SGPRT assay was performed.

231 For immunoblotting of proteins incorporated into lentiviral particles, the lentiviral particles-
232 containing supernatant was concentrated on sucrose cushion by ultracentrifugation at 50,000Xg

233 for 2 hours at 4°C¹⁴. Viral pellet obtained was resuspended in the Laemmli buffer containing
234 10mM TCEP as a reducing agent.

235

236 **SARS CoV-2 Genes and ACE2 expression**

237 To check the expression of ACE2 in ACE2-transduced HEK293T cells we isolated the RNA
238 from HEK293T and ACE2+ HEK293T cells using Trizol and synthesized cDNA from 1ug of RNA
239 using oligoDT primers obtained from both the cells. To quantify the level of ACE2 expression,
240 qPCR was performed using ACE2 specific primers 5'-GGGATCAGAGATCGGAAGAA-3'
241 forward and 5'-AGGAGGTCTGAACATCATC-3' reverse and GAPDH as control with primers 5'-
242 TGGAGAAGGCTGGGGCTCATTTGCA-3' forward and 5'-
243 CATACCAGGAAATGAGCTTGACAA-3'.

244 RT-PCR for SARS CoV-2 genes from the producer HEK293T cells was performed using the
245 forward primer 5'-TCCTACCCTCGTAAAGAATTC-3' and reverse primer 5'-
246 TCCGGACTTTTCAAACCTGCGGATGT-3' with the respective cDNA as template.

247

248 **Luciferase assay**

249 Luciferase assay was performed in 96-well plates to quantify level of transduction by spike
250 pseudotyped viral particles. Equal numbers of ACE2+ HEK293T cells were seeded in 96-well
251 plates (10,000 cells/well) 24h before transduction and incubated with the various pseudotyped
252 viruses for 48h. GFP cell count was scored using the SpectraMax i3X system (Molecular
253 Devices). Media was aspirated from each well after 48h and Cells were lysed by treatment with
254 100 µl lysis buffer for 20 minutes at room temperature. Luciferase readings were measured
255 using SpectraMax i3X by injecting 50 µl of substrate buffer in 50 µl of cell lysate in 96-well white
256 plates. Specifics of buffer composition may be found below in the section titled "Buffers and
257 common reaction mixtures".

258

259

260 **Western blotting**

261 For Western blot-based analysis, samples were prepared in a 4X Laemmli buffer, boiled for 5
262 min at 95°C, and run on either 8% or 12.5% tricine gels for electrophoresis depending upon the
263 molecular weight range being detected by this method. Following this, gels were electro blotted
264 on the PVDF membrane (Immobilon-FL, Merck-Millipore). Blocking of membranes was carried
265 out by incubation with either a 5% BSA solution or the proprietary Odyssey Blocking Buffer (LI-
266 COR Biosciences) for one hour, followed by both primary and secondary antibody incubations

267 for one hour each at room temperature, each of which were followed by three washes for five
268 minutes.

269 Detection of p24, beta actin, SARS CoV-2 spike glycoprotein, SARS CoV-2 genes, and ACE2-
270 IgFc was carried out using mouse anti-p24 (NIH ARP), rabbit anti-beta actin (LI-COR
271 Biosciences, Cat# 926-42210, RRID:AB_1850027), mouse anti-spike (Cat#ZMS1076, Sigma
272 Aldrich), mouse anti-Strep (Qiagen, Cat# 34850), and mouse anti-Histidine (Invitrogen, Cat#
273 MA1-21315), respectively, as primary antibodies. Secondary antibodies used were either IR dye
274 680 goat anti-mouse, IR dye 800 goat mouse, or IR dye 800 goat anti-rabbit (LI-COR
275 Biosciences Cat# 925-68070, RRID:AB_2651128, and LI-COR Biosciences Cat# 925-32211,
276 RRID:AB_2651127).

277

278 **Generation of a plasmid expressing synthetic ACE2-IgFc microbody**

279 Genomic DNA isolated from HEK293T cells using the Macherey Nagel Nucleospin kit
280 (#740952.50) was used as a template for PCR amplifying the Fc region of human IgG. The
281 forward primer 5'-CAGCACCTGAACTCCTGGGGGACCG-3' and reverse primer 5'-
282 CCTTTGGCTTTGGAGATGGTTTTTC-3' was used to amplify the first exon encoding the Fc
283 region. The forward primer 5'-AGGGCAGCCCCGAGAACCACAGGTG-3' and reverse primer 5'-
284 TTTACCCGGAGACAGGGAGAGGCT-3' was used to amplify the second exon encoding the Fc
285 region. Both fragments were individually amplified further using the combination of forward and
286 reverse primers as 5'-
287 GAAAACCATCTCCAAAGCCAAAGGGCAGCCCCGAGAACCACAGGTG-3' and 5'-
288 TATATATTCTAGATTAATGGTGATGGTGATGATGGCCGCCTTTACCCGGAGACAGGGA-3'
289 for the first exon's amplicon and 5'-
290 ATATATCTCGAGGACAAAACCTCACACATGCCACCGTGCCAGCACCTGAACTCCTG-3'
291 and 5'-CCTTTGGCTTTGGAGATGGTTTTTC-3' for the second exon's amplicon, respectively.
292 Finally, both these fragments were combined using the forward primer 5'-
293 ATATATCTCGAGGACAAAACCTCACACATGCCACCGTGCCAGCACCTGAACTCCTG-3'
294 and reverse primer 5'-
295 TATATATTCTAGATTAATGGTGATGGTGATGATGGCCGCCTTTACCCGGAGACAGGGA-3' to
296 generate the final Fc fragment, which was cloned into pTZ57R.
297 Addgene (#154987) was used as template for ACE2 amplification, using the forward primer 5'-
298 GAACAAGAATTCTTTTGTGGGA-3' and reverse primer 5'-
299 TTTGTCCTCGAGGGAAACAGGGGGCTGGTTAG-3' a 421 bp fragment of the same was
300 amplified and cloned into pTZ57R.

301 Using an EcoRI/XhoI digestion, the ACE2 fragment was combined upstream of the Fc, and the
302 combined construct was ligated into the ACE2 containing plasmid using a EcoRI/XbaI digestion
303 to yield the final ACE2-IgFc construct. The construct was verified with Sanger sequencing (refer
304 to “Table S2: Sequences of ACE2-IgFc”).

305

306 **Biochemical characterization of ACE2-IgFc microbody**

307 HEK293T cells were transfected with the plasmid encoding ACE2-IgFc (5 µg plasmid in a 35
308 mm dish). As a control, 5 µg of pcDNA3.1BS(-) was also transfected. Media was changed
309 twelve hours post-transfection and fresh DMEM (without FBS) was added to the dishes. Culture
310 media was collected both 48- and 72-hours post-transfection, and samples were prepared in
311 either 8% or 2% SDS-containing 4X Laemmli buffer (with and without TCEP added,
312 respectively) for SDS-PAGE. 8% tricine gels were run, and analyzed using Western Blotting.
313 The amount of ACE2 present in the supernatant was determined by comparison with standard
314 concentrations of pure BSA as ascertained by band density analysis following silver staining of
315 SDS-PAGE gels. For Western Blotting, the proteins were transferred to a PVDF membrane,
316 blocked in a 5% BSA solution in TBS, and primary mouse-derived anti-Histidine antibodies were
317 incubated with the blot in a 1:4000 dilution, followed by goat-derived anti-mouse antibodies in a
318 1:5000 dilution.

319

320 **Pull-down assay using ACE2-IgFc**

321 A 30 µl of protein-G Dynabeads (ThermoFisher Scientific Cat #10003D) were first equilibrated by
322 washing with 10% FBS-containing DMEM. Following this, these were incubated with gentle
323 mixing by inversion for 15 minutes with 100 µl of ACE2-IgFc containing supernatant (equivalent
324 of 10 µg/ml). This was split into three equal fractions of 10 µl each. The beads-containing
325 mixtures then were immobilized on a magnetic rack, supernatant was aspirated off, and
326 replaced with 100 µl (10mU equivalent/mL RT) of culture supernatant carrying either bald
327 viruses or viruses pseudotyped with VSV-G or Spike glycoproteins. Mixing was carried out for a
328 period of 15 minutes, following which these were placed back on the magnetic rack, supernatant
329 was aspirated, and the beads washed twice with SGPRT Core Buffer - first with 500 µl and
330 then with 100 µl. Finally, 20 µl of RT Lysis Buffer was added and the reaction was incubated at
331 room temperature before mixing with TritonX diluted 10-fold using core buffer. The resulting
332 supernatant was collected after immobilizing the beads and processed for an SGPRT Assay.

333

334 **Neutralization Assay**

335 To quantify the amount of ACE2-IgFc required to inhibit the infection in ACE2+ HEK293T cells,
336 we treated 100 µl of spike pseudotyped virus (normalised to RT units) with a variable amount of
337 ACE2-IgFc containing medium. The mixture was incubated for fifteen minutes at room
338 temperature, following which each sample was used to transduce ACE2+ HEK293T cells
339 seeded in 96-well plates. Image acquisition (CellInsight CX7 High Content Screening platform,
340 ThermoFisher Scientific) GFP cell count (Spectramax13 Molecular Devices), and luciferase
341 assay were performed 48 hours post-transduction, in the enlisted order.

342

343 **Software**

344 All graphs were generated using GraphPad Prism (version 9.0). Specific portions of images
345 were produced using Biorender.

346

347 **Acknowledgment**

348 This work was supported by the intramural funds, a Department of Biotechnology (DBT) grant
349 (BT/PR26013/GET/119/191/2017), and the Wellcome Trust/DBT India Alliance Fellowship
350 [grant number IA/I/18/2/504006 awarded to AC]. TM and PR are supported by a fellowship from
351 the MHRD. AC is a recipient of the Innovative Young Biotechnologist Award from the DBT.
352 Authors are grateful to Nevan Krogan, Massimo Pizzato, Jeremy Luban, Sonja Best, Raffaele
353 De Francesco, Didier Trono, Sunando Datta, and the NIH AIDS Reagent Program for the
354 reagents and cell lines.

355

356 **References**

357

- 358 1. Huang, Y., Yang, C., Xu, X., Xu, W. & Liu, S. Structural and functional properties of SARS-
359 CoV-2 spike protein: potential antivirus drug development for COVID-19. *Acta Pharmacol.*
360 *Sin.* **41**, 1141–1149 (2020).
- 361 2. Sreepadmanabh, M., Sahu, A. K. & Chande, A. COVID-19: Advances in diagnostic tools,
362 treatment strategies, and vaccine development. *J. Biosci.* **45**, 148 (2020).
- 363 3. Crawford, K. H. D. *et al.* Protocol and reagents for pseudotyping lentiviral particles with
364 SARS-CoV-2 Spike protein for neutralization assays. *bioRxiv* 2020.04.20.051219 (2020)
365 doi:10.1101/2020.04.20.051219.
- 366 4. Johnson, M. C. *et al.* Optimized Pseudotyping Conditions for the SARS-COV-2 Spike

- 367 Glycoprotein. *J. Virol.* **94**, (2020).
- 368 5. Neerukonda, S. N. *et al.* Establishment of a well-characterized SARS-CoV-2 lentiviral
369 pseudovirus neutralization assay using 293T cells with stable expression of ACE2 and
370 TMPRSS2. <http://biorxiv.org/lookup/doi/10.1101/2020.12.26.424442> (2020)
371 doi:10.1101/2020.12.26.424442.
- 372 6. Plescia, C. B. *et al.* SARS-CoV-2 viral budding and entry can be modeled using BSL-2 level
373 virus-like particles. *J. Biol. Chem.* jbc.RA120.016148 (2020) doi:10.1074/jbc.RA120.016148.
- 374 7. Shang, J. *et al.* Cell entry mechanisms of SARS-CoV-2. *Proc. Natl. Acad. Sci.* **117**, 11727–
375 11734 (2020).
- 376 8. Tandon, R. *et al.* Effective screening of SARS-CoV-2 neutralizing antibodies in patient
377 serum using lentivirus particles pseudotyped with SARS-CoV-2 spike glycoprotein. *Sci. Rep.*
378 **10**, 19076 (2020).
- 379 9. Hu, J. *et al.* Development of cell-based pseudovirus entry assay to identify potential viral
380 entry inhibitors and neutralizing antibodies against SARS-CoV-2. *Genes Dis.* **7**, 551–557
381 (2020).
- 382 10. Lei, C. *et al.* Neutralization of SARS-CoV-2 spike pseudotyped virus by recombinant ACE2-
383 Ig. *Nat. Commun.* **11**, 2070 (2020).
- 384 11. Tada, T. *et al.* An ACE2 Microbody Containing a Single Immunoglobulin Fc Domain Is a
385 Potent Inhibitor of SARS-CoV-2. *Cell Rep.* **33**, 108528 (2020).
- 386 12. Gordon, D. E. *et al.* A SARS-CoV-2 protein interaction map reveals targets for drug
387 repurposing. *Nature* **583**, 459–468 (2020).
- 388 13. Khorsand, B., Savadi, A. & Naghibzadeh, M. SARS-CoV-2-human protein-protein
389 interaction network. *Inform. Med. Unlocked* **20**, 100413 (2020).
- 390 14. Chande, A. *et al.* S2 from equine infectious anemia virus is an infectivity factor which
391 counteracts the retroviral inhibitors SERINC5 and SERINC3. *Proc. Natl. Acad. Sci.* **113**,
392 13197–13202 (2016).

- 393 15. Banerjee, A. K. *et al.* SARS-CoV-2 Disrupts Splicing, Translation, and Protein Trafficking to
394 Suppress Host Defenses. *Cell* **183**, 1325-1339.e21 (2020).
- 395 16. Flower, T. G. *et al.* Structure of SARS-CoV-2 ORF8, a rapidly evolving coronavirus protein
396 implicated in immune evasion. *bioRxiv* 2020.08.27.270637 (2020)
397 doi:10.1101/2020.08.27.270637.
- 398 17. Schubert, K. *et al.* SARS-CoV-2 Nsp1 binds the ribosomal mRNA channel to inhibit
399 translation. *Nat. Struct. Mol. Biol.* **27**, 959–966 (2020).
- 400 18. Xia, H. *et al.* Evasion of Type I Interferon by SARS-CoV-2. *Cell Rep.* **33**, 108234 (2020).
- 401 19. Carlson, C. R. *et al.* Phosphoregulation of Phase Separation by the SARS-CoV-2 N Protein
402 Suggests a Biophysical Basis for its Dual Functions. *Mol. Cell* **80**, 1092-1103.e4 (2020).
- 403 20. Weissman, D. *et al.* D614G Spike Mutation Increases SARS CoV-2 Susceptibility to
404 Neutralization. *Cell Host Microbe* **29**, 23-31.e4 (2021).
- 405 21. Zhang, L. *et al.* SARS-CoV-2 spike-protein D614G mutation increases virion spike density
406 and infectivity. *Nat. Commun.* **11**, 6013 (2020).
- 407

408
409
410
411
412
413
414
415
416
417
418
419
420
421
422
423
424
425
426
427
428
429
430
431
432
433

Figure Legends

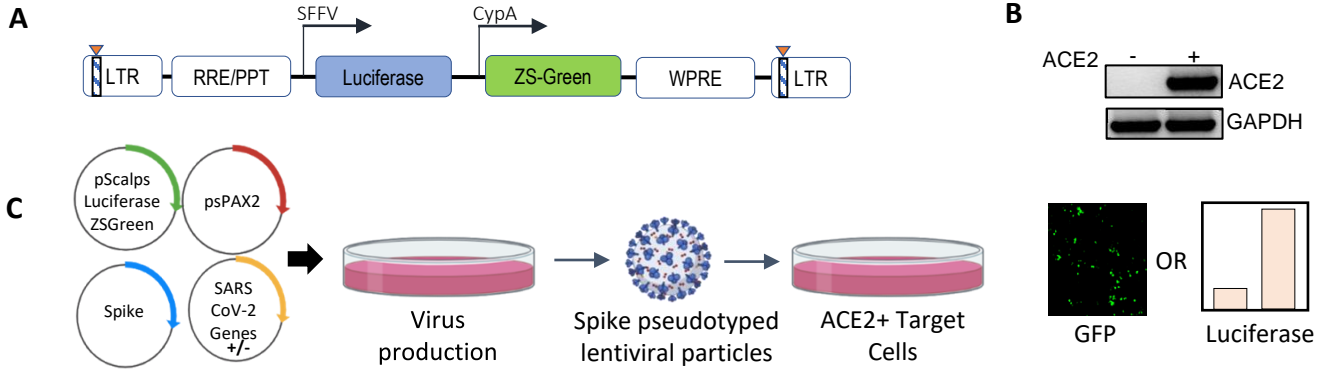
Figure 1. Experimental setup and constructs. (A) Schematic representation of the pScalps Luciferase ZsGreen lentiviral reporter construct. (B) ACE2 expression from the hygromycin selected HEK293T cell line transduced with a ACE2 gene carrying lentiviral vector. (C) Schematic depiction of the SARS CoV-2 genes' screen. Transfection with an empty vector served as control. Readout from the screen was obtained in the form of firefly luciferase activity or GFP-positive cell count.

Figure 2. SARS CoV-2 N enhances lentiviral spike-particle infectivity. (A). Results from the screen of SARS CoV-2 genes, either by quantifying luciferase activity (left panel) or GFP positive cell count (right panel). Vector normalized values for both readout methods has been shown, such as to indicate the percentage change relative to the baseline (indicated by the dotted line) $n=4 \pm SD$. (B) Expression of each of the SARS CoV-2 genes was verified by RT-PCR and (C) Western blotting depicting the p24 levels from the virus-producing cells. Actin served as loading control. (D) Microscopy images for the infected cells with indicated conditions (scale 100 μM). (E) Empty vector normalized Luciferase readout for VSV-G pseudotyped lentiviral particles. $n=4 \pm SD$.

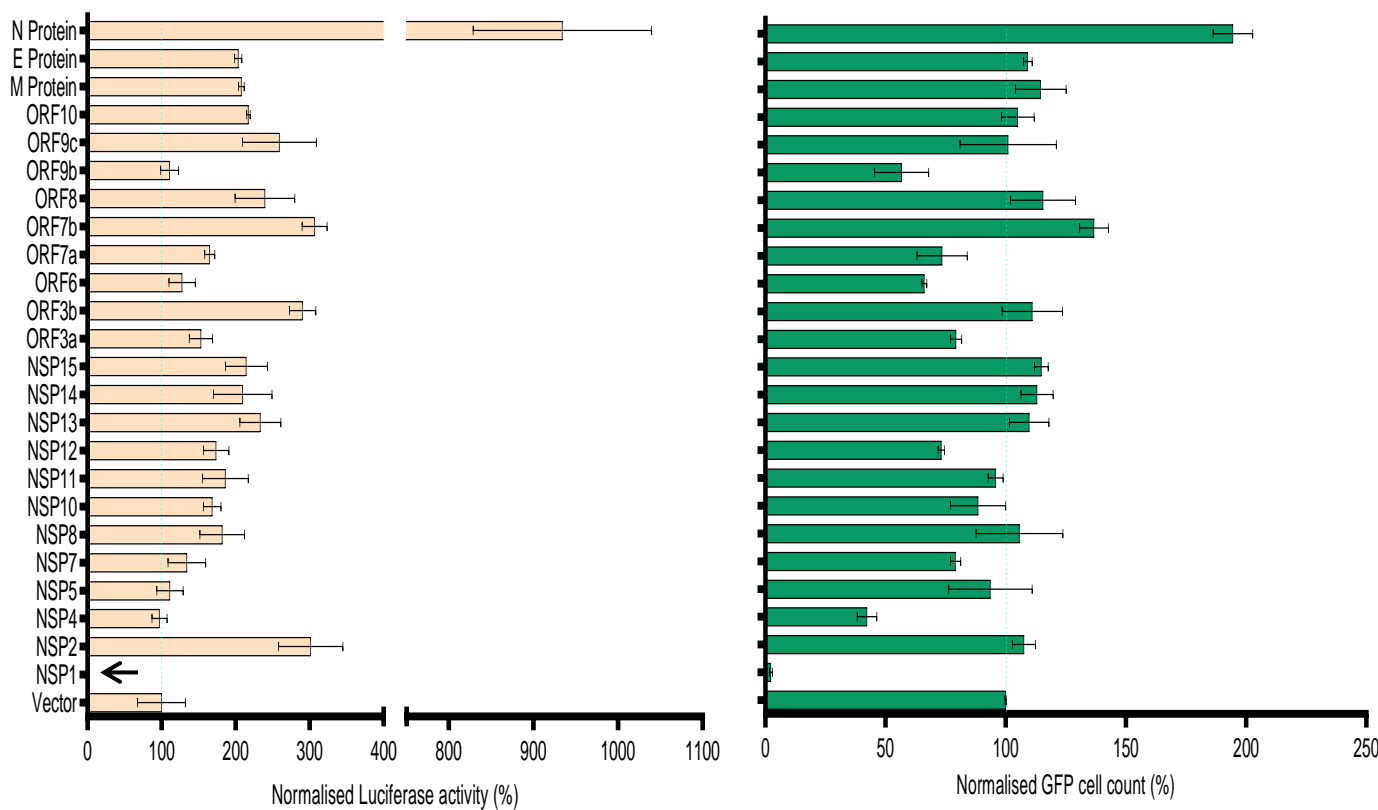
Figure 3. Characterization of the ACE2-IgFc microbody. (A) Schematic of the ACE2-IgFc neutralizing microbody. (B) Effect of a reducing agent (TCEP) on the migration of ACE2-IgFc on the gel. Anti-His antibody indicating monomeric vs dimeric states of the protein visualized by western blotting from the cell culture supernatant. (C) Protein G-bound ACE2-IgFc and the enrichment of virus particles. The RT activity of the input VSV-G or Spike particles was normalized to the no-envelope particles, set to 100%. $n=3 \pm SD$.

434 **Figure 4.** Neutralizing effects of ACE2-IgFc on the N-enhanced spike lentiviral particles and
435 biochemical characterization of the virions (A) Neutralization assay using ACE2-IgFc pre-
436 treated lentiviral particles with indicated amount of ACE2-IgFc (on the x-axis) for the
437 lentiviral particles produced in the presence of indicated genes. The particles were
438 normalized to the reverse transcriptase units obtained from the SGPRT assay before
439 addition to target cells. Luciferase activity obtained from non-enveloped particle transduction
440 was considered as baseline. The lines represent extent of residual infectivity (expressed as
441 x-fold), post-treatment of ACE2-IgFc, with respect to N-exclusive particles $n=3 \pm SD$. (B)
442 Biochemical analysis of the virus particles and the corresponding cell lysates. The viral
443 proteins were visualized by western blotting using antibodies raised against S2 domain of
444 SARS CoV2 spike. The N protein and p24 were detected using Anti-Strep tag and anti-p24
445 antibody, respectively. Actin served as loading control.
446
447

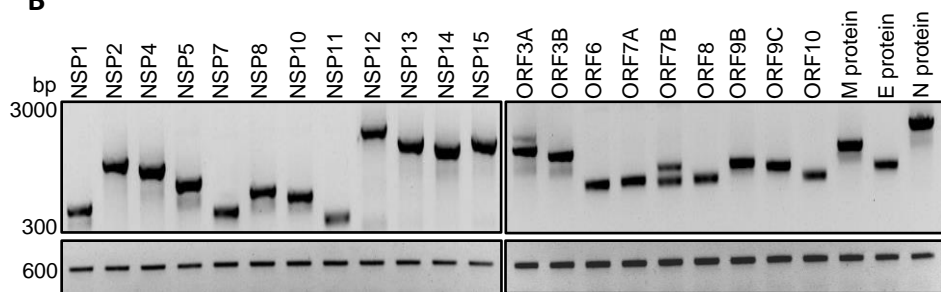
Fig-1



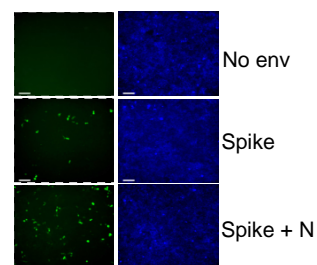
A



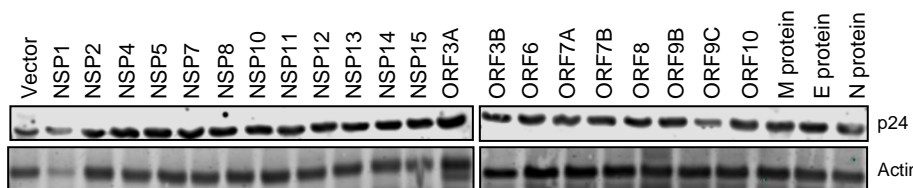
B



D



C



E

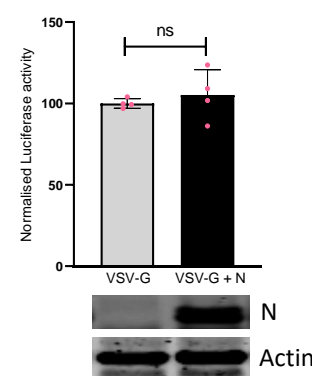


Fig-3

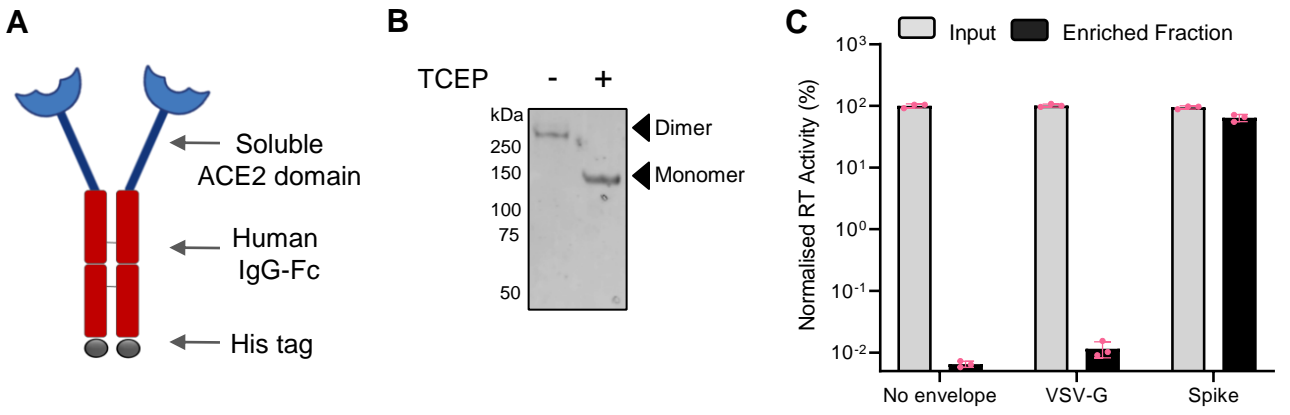


Fig-4

